I-V Mode Integrated Droop PI Controller for Automotive LED Applications

K. Subha Sharmini, K. Vijayakumar

Electrical and Electronics Engineering Department, SRM Institute of Science and Technology, Chennai, 603203 INDIA (Tel: 91-9443581662; e-mail: subha.a.star@ gmail.com).

Abstract: Light-Emitting Diodes (LED) lights are the most economical choice of lighting schemes in terms of lumens per Watt and several other factors compared with their traditional counterparts. This paper used control theory to model, simulate and analyze an LED driver adapted from the idea of synchro-droop cascaded PI controller (CDPI) used in its reduced DC form. The control method is applied to all the classic non-isolated versions of DC-DC converters. Their behavior is then investigated in the time domain to prove its supremacy against a conventional PI controller (CPI). The simulation results obtained for these configurations under voltage and current control modes (I-V) show the efficacy of a boost converter as the topology, CDPI as the control technique, and boost as the gain mode. Among the basic DC converter topologies, the boost converter seems less affected by multiple disturbances in the line, reference voltage, and LED load transient changes with the CDPI control than with its single-stage CPI counterpart. Experimental analysis using a prototype hardware model powering up a 24/30 V, 200 mA, 27 W LED automotive dual string lamp load agree with the simulation results.

Keywords: Control, Converters, DC Droop, PI, LEDs.

1. INTRODUCTION

Ten to twenty per cent of the world's electrical energy is consumed by powering up lighting load arrangements to illuminate public and private spaces indoor and outdoor, commercial and residential. Such lighting schemes fall under traditional and non-traditional varieties. Incandescent, fluorescent, mercury, and sodium vapour lamps have been in existence since the early days of electric lighting. While incandescent bulbs and fluorescent tubes are popular for residential use, street lighting systems were traditional mercury or sodium vapour. CFLs (Chloro fluorescent lamps), LEDs and solar lights are new technologies that are fast catching up to their place in the modern world. The considerable advantages of LEDs make them the people's choice: 1) their absence of harmful gases and, hence greenness; 2) durability and longevity of life; 3) colour options and good colour rendering index; 4) appreciable luminous efficacy, etc. Their good photometric properties lead to their utility in a large number of applications: 1) vehicular; 2) decorative lighting; 3) advertising panels; 4) traffic lights; 5) television; and 6) general lighting. The power rating for traffic lights is low, and for street lighting applications, the power should be medium to high. LED systems should satisfy the power factor (PF), total harmonic distortion (THD), and other standard requirements that are generally set by international regulatory authorities. A driver circuit is necessary to meet the above standards and keep a constant current to the LED load.

(Wu et al., 2018) presented an LED driver's design and analysis with carrier disposition control and a dual-output front end converter. In (Alonso et al., 2017), the authors outlined steady-state and dynamic response of a variable – inductor based driver current control of multiple LED arrays with short circuit and open circuit protection without a downstream converter. In (Mujjalinvimut et al.. 2016) the authors experimented with an analogue control strategy with a gain feedback compensator and an adaptive feed-forward loop. The former minimized the effect of duty cycles on the system gain and the latter for mitigating the ripple. In (White et al., 2015), the authors presented a simple control technique with the peak duty cycle control method implemented within an average current modulator for a single-stage PFC (Power Factor Corrector) LED driver for the reduction in output current ripple and energy storage capacitance. The authors of (Wang et al., 2014) introduced a novel method to improve LED dimming flexibility by switch regulating the inductor current pulse width modulation (PWM) pulses during the dimming period for a current –controlled buck converter operating in discontinuous mode. The authors of (Moon et al., 2013) presented a new pulse duty control frequency modulation method for an interleaved single-stage fly-back AC-DC converter resulting in high efficiency under both heavy and light loads, wider input voltage, high PF, and decreased THD. The authors of (Lamar et al., 2009, 2008) presented an experimental analysis of high-frequency peak current mode control with compensation ramp selection as the control voltage for boost, fly-back, SEPIC and zeta PFC stages.

Generally, LEDs are DC loads, unlike other forms of lighting. An available AC supply usually powers LEDs after rectification and conversion conditioning. The control presented in this article aims to eliminate this dependence on AC and utilize available renewable energy resources or batteries in the case where LED lighting loads are used for vehicular applications/small scale rural household lighting. Nowadays, the batteries used in vehicles are popular leadacid batteries typically rated around 12 V and supplying energy to all auxiliary lighting units. Battery DC/DC LED drivers are available in different packages with varying converter configurations and control modes. However all the control elements are single-loop integral or PI regulators that are slow in regulating output voltage and current in response to the battery voltage changes. A simplified droop-cascaded dual PI structure (CDPI) is proposed to improve the steady-state/ transient response. Droop is added in as part of the control schematic to achieve the appropriate current sharing amongst automotive LED lights (Headlights, sidelights, brake and tail lights) that are parallel wired for 48 V and switched ON-OFF under transitory dynamic conditions.

Experimental results establish that droop with voltage mode feedback control shows good dynamic behaviour and quick stabilization even when subjected to simultaneous disturbances in the line and load side compared to a conventional single-stage PI (CPI) controller without droop. This paper is organized as follows: LEDs, their typical driving methods and modelling are reviewed in section 2. Section 2 also presents a brief design procedure for the fundamental transformer-less topologies and the control methodology. The results and discussion of the simulation and experimental runs are given in section 3.

2. CONVERTER, CONTROL AND LED LOAD MODELING

Fig.1 shows the DC LED driver's general block diagram representation interfaced to the parallel wired LED string light loads with a DC-DC converter (non-isolated types) and controlled with a set of composite controllers. Non-isolated converters are preferred due to the absence of expensive and lossy transformer. The following controllers are integrated to form the mixed controllers for comparative analysis:

- CPI-Traditional single-loop PI with voltage(V) and current mode (I) controls (shown)
- CDPI-Cascaded dual-loop PI with voltage(V) and current mode (I) controls (shown)

Given below is the brief modelling of all modules.

2.1 LED Load Model

An LED is a special solid-state PN diode, without silicon. The lower energy barrier value of silicon makes it unsuitable for electroluminescence. Present-day LED drivers rely mostly on AC supply for its excitation, as electrical energy is typically generated in its alternating form. Such AC drivers have to rectify, maintain standard levels of line side PF and reduce electromagnetic interference. The end-stage DC-DC converters should change the pulsating DC to a constant DC to suit the LED loads. Generally, LED drivers in their traditional form may be single, dual or integrated stage types. This categorization is based on how the power factor corrector circuits and DC-DC converter are used. In a single-stage driver circuit, the same circuit is used for PFC and conditioning. Although the circuit is simple, it needs a large storage capacitor. In a dual-stage arrangement, independent power circuits used for PFC and DC conditioning lead to high circuit complexity with many components. In recent years, many modern integrated stage LED drivers have been developed to share switches and control.

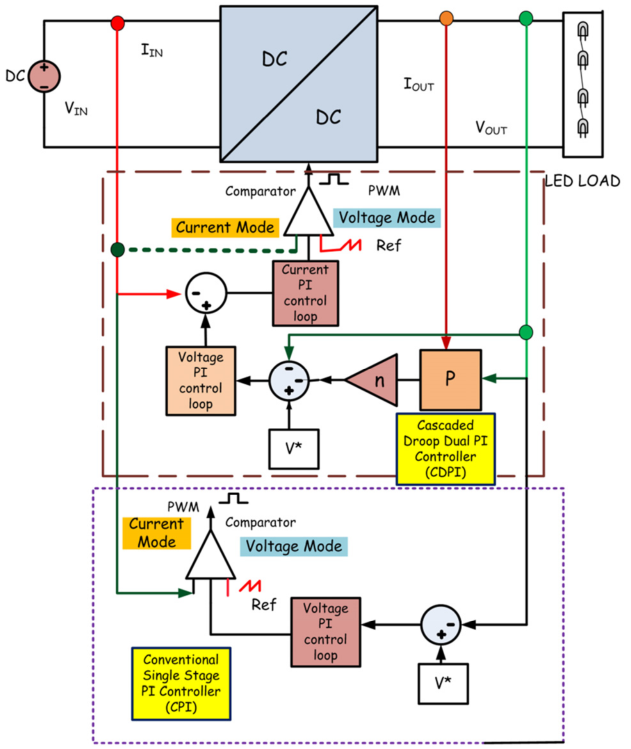

Fig. 1. Control Schematic showing CPI and CDPI controllers.

The various characteristic parameters of LEDs, i.e. the forward voltage drop, internal energy barrier, the temperature, the colour, and the wavelength, are all inter-related (Winder, 2008). In particular, the voltage drop varies proportionally with the current. As a part of passive control, a small value of equivalent series resistance (ESR) as a series addition is necessary with the constant voltage load representation, given by the ratio between the increase in forward voltage drop and the current.

Zener diodes in series with a small ESR value could be used as an equivalent dummy to simulate an LED load as both represent constant voltage loads. The Zener reverse voltage will be slightly greater than the forward voltage drop (V_f) of an LED. A small difference in values exists between their dynamic impedance and power ratings. The ESR should also be chosen to be a slightly higher value. A 4 W, 3.9 V Zener diode could be used to replace a white LED. Fixing up the voltage drop tolerance between 2.4 to 5.4 V, and 200 mA current, 13 Zener diodes representing LEDs are chosen to be in series in a single string for boost mode. The ESR is to be 15 Ω for each LED, or the total external resistance is 200 Ω as per the formula shown below:

$$ESR = \frac{V_{IN\,min} - V_{f\,max}}{I_{OUT\,min}} \tag{1}$$

Table. 1 lists the necessary criteria for designing the DC droop based LED driver. Fig. 2 shows the simulation dummy equivalent and the X-Y plots (I-V and P-I curves) of a single LED model run in MATLAB simulation.

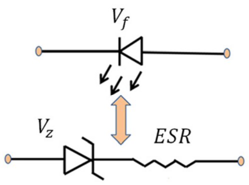

Fig. 2(a). LED dummy simulation model.

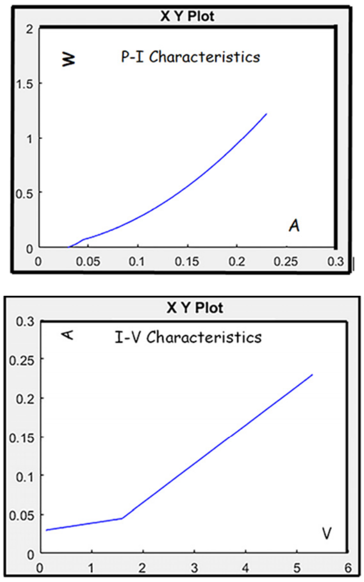

Fig. 2(b). P-I and I-V curves.

Table 1. Converter design criteria.

Criterion	Value
Line Voltage	9-15 V
LED Current	350 mA (max)
Allowable Current Ripple	10 %
LED Voltage	40-50 V
Switching Frequency	10 KHz
Efficiency	90 %

2.2 Converter Design in Brief

Boost, buck, buck-boost (BB), CUK, zeta and SEPIC converters as configured in Fig.3 do not have transformer isolation and are very basic and famous circuit topologies of DC conditioning. These converters could take the place of switching LED drivers. A buck-based driver becomes an attractive choice for low-voltage, high-brightness LEDs as they can operate with high efficiencies.

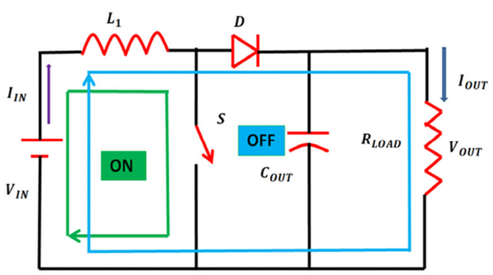

Fig. 3(a). Boost Converter.

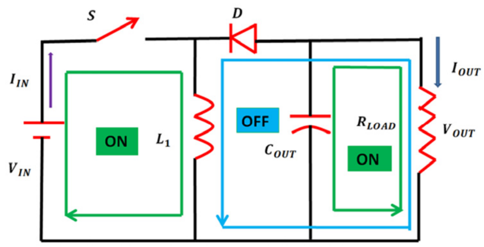

Fig. 3(b). Buck-Boost Converter.

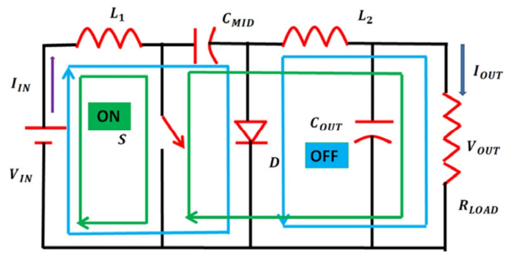

Fig. 3(c). CUK Converter.

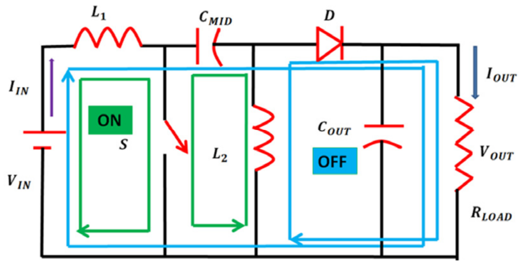

Fig. 3(d). SEPIC Converter.

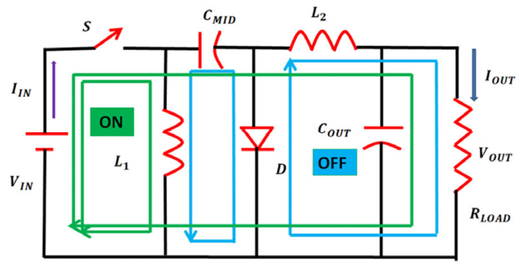

Fig. 3(e). Zeta Converter.

Boost converters are preferable when the input to output voltage ratio is greater than 1.5. However, when it comes to automotive applications, where a single driver is favourable to cover a wider range of voltage, buck-boost, CUK or SEPIC circuits should be chosen (Winder, 2008; Czarkowsk, 2010; Basso, 2003; Rashid, 2003; Erickson, 2001). Table. 2 give the design values of the above-mentioned converters with reference to the Texas application reports and manuals.

Table 2. Converter circuits- Design reference.

	C_{MID}	L_1	L_2	C_{OUT}
CUK	67 µF	4.5 mH	3.5 mH	220 µF
Zeta	150 µF	22 µH	22 µH	220 µF
BB	-	9.6 mH	-	50 µF
Boost	-	2.3 mH	-	50 µF
SEPIC	150 µF	22 µH	22 µH	500 µF

2.3 Control Methodology

Over the years, many control techniques have been used to maintain the constancy of LED load-side parameters. Voltage mode, (Li et al., 2012; Mammono, 1999) current mode (Aroudi et al., 2021; Chen et al., 2020), and hysteresis control methods compose the basic feedback control strategies for switching regulators. Each of these types has its own merits and demerits, and a suitable method must be chosen after careful consideration of these factors. In this paper, a droop control method in its reduced form controls the converters' under-voltage mode and current mode. Droop (Zhang et al., 2021) is a common term linked with the conventional running of alternators in parallel synchronism (Ghanbari et al., 2020; Kannan et al., 2016; Zhong et al., 2013).Sudden overloading results in a mismatch between the mechanical power input and the electrical power output.

$$V_{OUT} = V^{*} - nP \quad (2)$$

$$\omega_{OUT} = \omega^{*} - mQ \quad (3)$$

where (ω_{OUT} - ω^*) (V_{OUT} -V^*) represent the frequency and the voltage magnitude deviation; *m, n*, represent the droop gain, *P, Q* , represent the real and the reactive power (Subha, 2019). As per the above two droop relations (resistive nature), the power/load mismatch will be automatically corrected by simultaneous changes in the prime mover's speed (frequency) and voltage magnitude. These relations can be electronically implemented in the form of a control loop for power electronic interface units (inverters, DC converters) coupling the source to the grid/load (Peyghami et al., 2017). Voltage regulation (Peyghami et al., 2017) is achieved by injecting a very small AC voltage into the DC voltage reference (frequency injection) to operate the micro sources in parallel.

This article propose implementing the droop control in a more reduced form (resistive nature) by eliminating the Q Vs. ω frequency droop relation since the DC converters operates in non-parallel mode, feeding only LED loads. The control approach (Fig.1) is to share current proportionally between LED strings that may be connected in parallel at different times (switching ON and OFF of LED lights in moving vehicle) achieved by controlling the DC output voltage (Braitor et al., 2021) by output power (P Vs. Voltage). The cascaded droop dual PI loop structure follows equation (2). Voltage control forms the outer master loop and the control of the current, its inner slave stage. The mathematical formulation given below gives the modulating signal for the CDPI control loop:

$$M(S) = \{(V^{*} - V_{OUT} - nP)\, G_V(S) - I_{OUT}(S)\}\, G_I(S) \quad (4)$$

$$G_V(S) = \{K_{PV} + \frac{I_{IV}}{S}\} \text{ - Master loop gain} \quad (5)$$

$$G_I(S) = \{K_{PI} + \frac{I_{II}}{S}\} \text{ - Slave loop gain} \quad (6)$$

2.4 Tuning of Control Parameters

For control engineers, tuning the PID structures is quite difficult as they are interrelated with the system's stability, transients, and dynamics. There are several techniques used over the years for tuning. One of the popular heuristic rules that practically recommend good values is the Ziegler-Nichols rule. The mathematical procedures do not require an accurate system model and hence it is the most implemented technique. While the Zieger Nichols algorithm outlines an initial estimation of the gains, further fine-tuning is required to result in an excellent controller design.

Ziegler-Nichols deduced two methods with simple math formulas based on the step responses of the system. The reaction curve method is usually for first-order cascaded systems without poles at the origin/complex poles at the origin, with S-shaped responses and zero overshoot. However, the second law is for higher-order systems that can be made unstable and, hence, selected to design the composite controller's gains and time constants, as discussed below:

- The derivative and integral constants are set to 0 and infinity.
- The proportional gain is increased gradually from zero to the critical value (*Kcr*), at which the response begins to oscillate.
- Calculation of the period of oscillation (*Pcr*) from the step response as shown in Fig. 4.
- The control parameters are roughly estimated and fine-tuned by trial and error.
- The transfer function representation of a PI controller is thus formulated as 0.45 *Kcr* {1+(1/0.83 *Pcr* S)

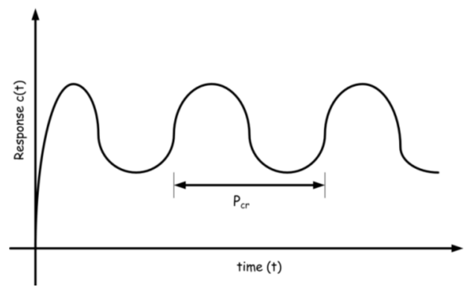

Fig. 4. Period of Oscillation (*Pcr)* from output response.

For instance, the critical gain (*Kcr*) values and the time period of sustained oscillations *(Pcr*) observed from the closed-loop step response curves of the boost converter are as tabulated in Table 3 for the single-stage and cascade PI controllers. Table. 4 gives the values of the proportional gain constants, and integral time constant for the voltage (K_{PV} *and* T_{IV}) and the current control(K_{PI} *and* T_{II}) loops of the cascaded droop PI controller (CDPI) and its conventional single-stage equivalent (K_P *and* T_I). The control is applied to the entire set of transformer free topologies of DC converters (Boost, Buck-Boost, CUK, SEPIC, and Zeta) with voltage and current mode controls integrated. The observations based on the comparative analysis between CDPI and CPI techniques in terms of response and step perturbation in the line and load side are summarized in the following sections.

Table 3. Values of *Kcr and Pcr.*

Controller Type	K_{cr}	P_{cr}
Single-Stage PI	1.55	0.0084
Cascaded Dual PI (Slave Loop)	0.1111	0.003
Cascaded Dual PI (Master Loop)	1	0.27

Table 4. Control design parameters.

Controller	Parameter	Value
(CPI)	$I = K_P/T_I$	10
(CPI)	K_P	0.7
(CDPI)	K_{PV}	0.45
(CDPI)	K_{PI}	0.05
(CDPI)	$I_{IV} = K_{PV}/T_{IV}$	20
(CDPI)	$I_{II} = K_{PI}/T_{II}$	2

3. SIMULATION AND EXPERIMENTAL RESULTS

Controllers are applied to the transformer-less versions of the traditional boost-based DC converters (Boost, Buck-Boost, CUK, SEPIC and Zeta) to evaluate their viability. The controller parameters are unchanged for all. A 15/48 V boost ratio with a 200 mA single LED string load consisting of 13 LEDs in series is chosen for the simulation runs. The observations are compared with a conventional PI controller, and the converter and the control with better performance indices were picked for the LED drivers (see Fig.5 and Fig.6).

3.1 Voltage Mode Integrated Boost Operation

For the same simulation set up, the zeta converter showed unacceptably large overshoots for both current and voltage and is eliminated from the choice options. The CUK and buck-boost converter voltages settled at 44 V below par compared with the set reference of 48 V for a conventional PI controller. The currents also showed poor flow, and so they were not considered for the driver. The boost converter proved to be the most effective circuit with its fast and smooth settlement to the final value of 48 V. The current had a 2 % ripple range (0.18 -0.2 A).

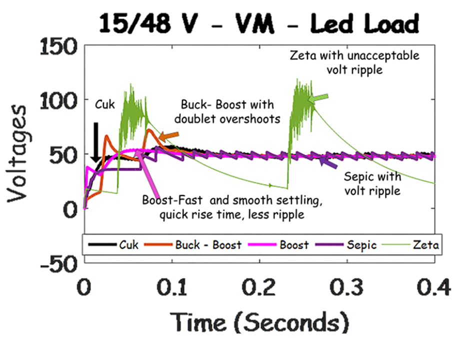

Fig. 5(a). Voltage waveforms of all DC-DC converters (CDPI-VM).

The second most favourable choice under-voltage mode is the SEPIC converter, but the ripple was slightly higher at about 5 % for voltage and 3 % for current. When run with a conventional PI, the boost and SEPIC circuits had a delayed settling time compared to the droop control. Droop control runs showed initial overshoots of meagre magnitude (Fig.5).

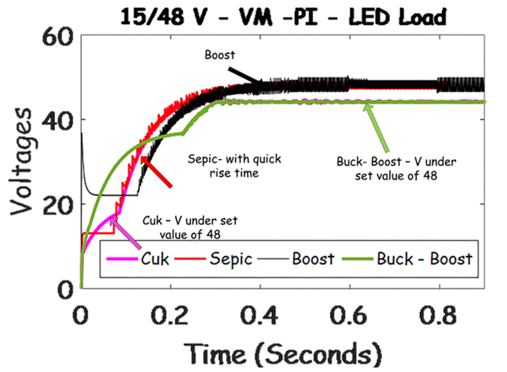

Fig. 5(b). Voltage waveforms of all DC-DC converters (CPI-VM).

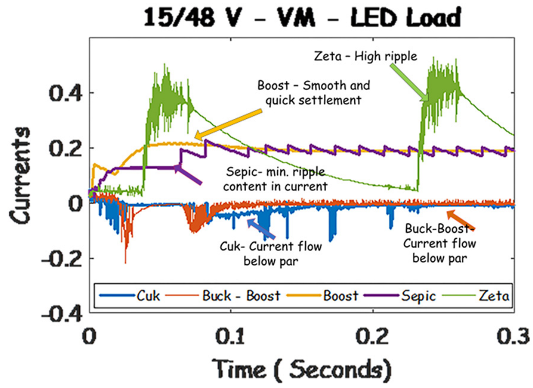

Fig. 5(c). Current waveforms of all DC-DC converters (CDPI-VM).

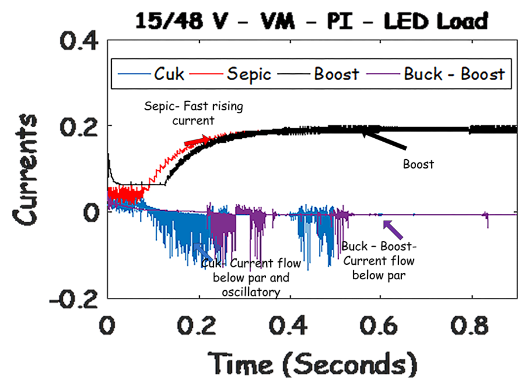

Fig. 5(d). Current waveforms of all DC-DC converters (CPI-VM).

3.2 Current Mode Integrated Boost Operation

Zeta is found again to be unstable, even under current mode PI and the droop based cascaded PI. Buck-boost had initial double overshoots in its voltage. Despite the CUK's and buck-boost converter's voltage settling well at 48 V, their currents exhibited oscillatory behaviour. The SEPIC converter is not able to reach the final value of the reference voltage in both cases. Under current mode too, the boost converter's performance is good in terms of ripple, and the final value is reached in a quicker time for the droop based cascaded PI controller than for the conventional (Fig.6).

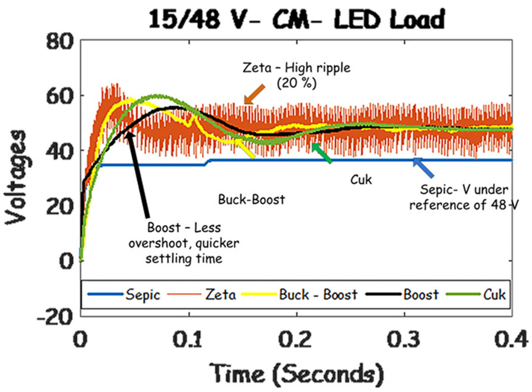

Fig. 6(a). Voltage waveforms of all DC-DC converters (CDPI-CM).

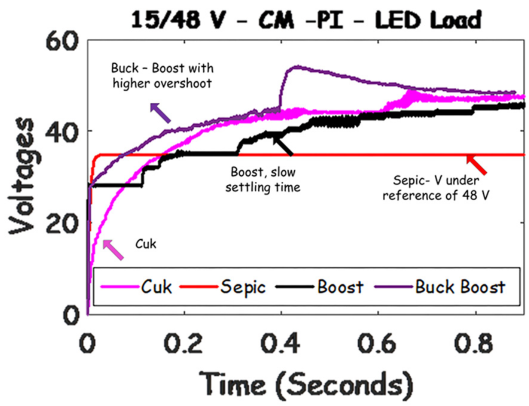

Fig. 6(b). Voltage waveforms of all DC-DC converters (CPI-CM).

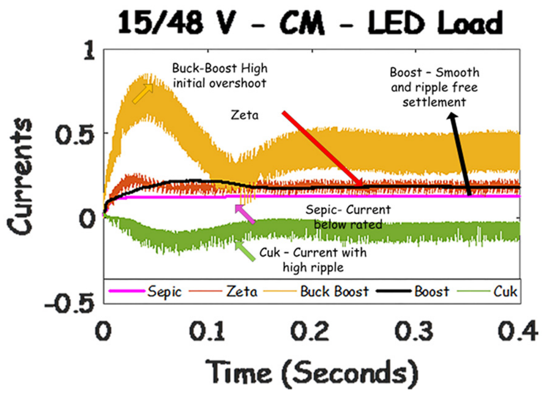

Fig. 6(c). Current waveforms of all DC-DC converters (CDPI-CM).

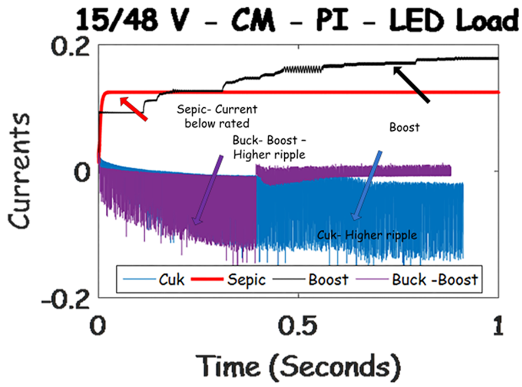

Fig. 6(d). Current waveforms of all DC-DC converters (CPI-CM).

3.3 Multiple Perturbation Analysis

The controller's performance and the closed-loop system when subjected to multiple perturbations is investigated in detail for the same variation in the line voltage and reference voltage for the converter (boost) found to be the best in the time domain. Step increments of (9-15) V at time *t*= 0.6 seconds in the line voltage along with a change in reference of 30 to 48 V at *t*= 1 second were induced as simultaneous disturbances , and the voltage line regulation is analysed for the cascaded droop PI controllers and the conventional PI controllers with constant load conditions.

The conditions of reference voltage changed from 30 to 48 V for the boost converter operated under CDPI-current mode (CM) alone were run at *t*=0.3 seconds to show diversity in the simulation set up (Fig.7). The time-domain behaviour of the converter with VM-CDPI is observed superior to CM-CDPI. Under current mode, the step incremental disturbance of line voltage at 0.6 seconds results in a higher overshoot compared to voltage mode. CPI-CM shows delayed and fluctuating settlement to the set reference and CPI-VM operation, voltage and current output with ripple.

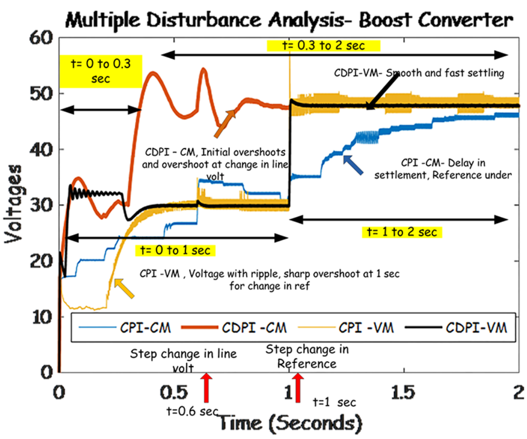

Fig. 7. Line and load voltage regulation for a boost converter controlled by CDPI and CPI (I-V Modes) –Without load dynamics.

3.4 Load Transients and Current Sharing Under Multiple Disturbances

The load voltage regulation characteristics and the current sharing behaviour of the CDPI controller fed LED string load for varying load conditions are discussed in this section with the multiple step change disturbances in the source and reference voltage retained. Step increments of (9-15 V) at time *t*= 0.6 seconds in the line voltage along with a change in the reference of 30 to 48 V at time *t*= 0.3 seconds were induced. A 13 LED string series load included in addition to the existing LED string at time *t*= 0.4 seconds gave the following observations shown in Fig.8. The results show the conventional single-stage PI controller's inability to regain stability after the induction of the load changes and other dynamic changes in the input side.

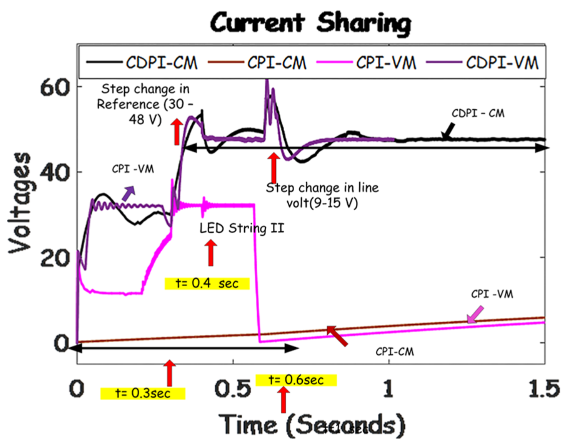

Fig. 8(a). Line and load voltage regulation for a boost converter controlled by CDPI and CPI (I-V Modes) –With load dynamics.

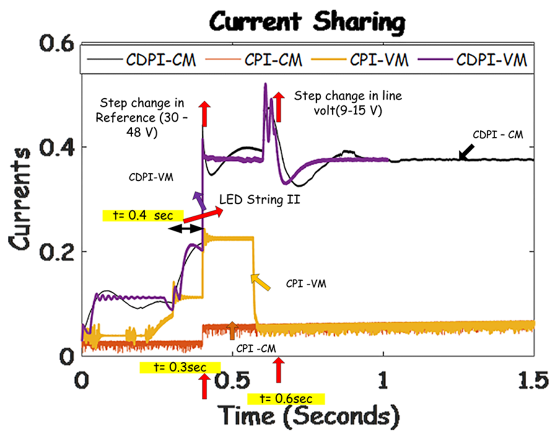

Fig. 8(b). Current sharing and regulation for a boost converter controlled by CDPI and CPI (I-V Modes) –With load dynamics.

3.5 Results and Discussion

Table. 5 presents the numerical measures of the basic DC converter performance metrics that indicate the reach and recovery to steady-state under the three experimental scenarios of case-I, II and III

Case-I: Under normal operating conditions without any transients or disturbances

- The steady-state error is approximately equal to 0, and the reference set value is reached 40 % fast for CDPI-VM than CDPI-CM, CPI-I, V Modes.

Case-II: System operation with line voltage changes only

- Reference tracking (both 30 and 48 V) is achieved for all controllers.
- With line side voltage changes from 9 to 15 V, transient overshoots were temporarily observed for all controllers. However, for CDPI-VM, an almost zero instant recovery with 1 % spiking is observed compared to 0.9:0.8 sec recovery for CPI-CM: CDPI-CM. All the controllers were able to recover to stable steady-state reference.

Case-III: System operation with line voltage changes and load dynamics

- While the CPI-CM controller did not reach the set reference of 48 V, CPI-VM has an 18 % steady-state error. With the line voltage change, the voltage dropped to zero. The current sharing between the added LED string loads is inaccurate.
- Although CDPI controllers integrated with voltage and current control modes showed 10 % temporary overshoots, the recovery time is 25 % faster for CDPI-VM.
- The dynamic parallel wiring of additional LED strings drew accurate current for CDPI-V, I modes

3.6 Experimental Analysis

The boost converter's simulation results with the CDPI controller integrated with voltage and current mode were further validated with OPAL's OP4510 HIL simulator and TP1470 data board. The current waveforms through the capacitor, boost inductor, switch and the voltage across the inductor obtained for both the operation modes are shown in Fig. 9 and Fig.10. Step disturbances are introduced at times *t*= 9 seconds and *t*= 10 seconds in the reference voltage and the input DC voltage, with the second LED string switched ON at *t*= 7 seconds to correlate with the simulation conditions.

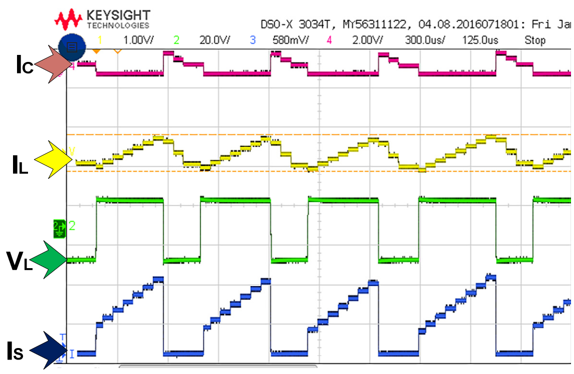

Fig. 9. Experimental waveforms for current mode integrated droop driver: Currents through capacitor (IC), inductor (IL), switch (IS) and voltage across inductor (VL).

Table 5. Steady-State, Transient and Dynamics.

		CPI-CM	CPI-VM	CDPI-CM	CDPI-VM
Case-I*	e_{ss}/t_s	8% (0.25 sec)	0% (0.25 sec)	0% (0.26 sec)	0% (0.1 sec)
Case-II**	**Ref. track (30 to 48 V at t= 1 sec)**	Yes	Yes	Yes	Yes
	Line Transients (9-15 V at t=0.6 sec)	5 % Overshoot, Recovery at t= 0.9 sec	4 % Overshoot, Ripple in Outputs	7 % Overshoot, Recovery at t= 0.8 sec	1 % Overshoot, Recovery at t=0.62 sec
Case-III***	**Ref. track (30 to 48 V at t= 0.4 sec)**	No	Yes (18 % e_{ss})	Yes (3 % e_{ss})	Yes (0 % e_{ss})
	Line Transients (9-15 V at t=0.6 sec)	No	Sharp Droop with No Recovery	10 % Overshoot, Recovery at t= 0.8 sec	10 % Overshoot, Recovery at t= 0.65 sec
	Load Dynamics (Parallel Addition of LED Load at t= 0.3 sec)	No	30V(1/2 Strings) (0.05A/0.12 A) and 48 V (2Strings) (0.22 A drawn)	30V(1/2 Strings) (0.12A/0.23A) and 48 V (2Strings) (0.4 A drawn)	30V (1/2 Strings) (0.12A/0.23A) and 48 V (2Strings) (0.4 A drawn)

*__Case-I__ (Performance with no transients or load changes for boost driver with all controllers)
**__Case-II__ (Performance with line transients only for boost driver with all controllers)
***__Case-III__ (Performance with line transients, and load dynamics)
Steady state error - e_{ss} and settling time - t_s

Fig.12 and Fig.13 shows the effectiveness in the controller fed driver's transient and dynamic performance The second LED string's addition results in the change of currents from 0.13 A to 0.2 A proving accurate sharing of currents. A laboratory prototype of the automotive dual string LED driver rated at 12 to 24/30 V (input to output voltage ratio), 200 mA current has also been built to confirm with the simulation results (see Fig.11). Each LED in the string is rated at 2 W.

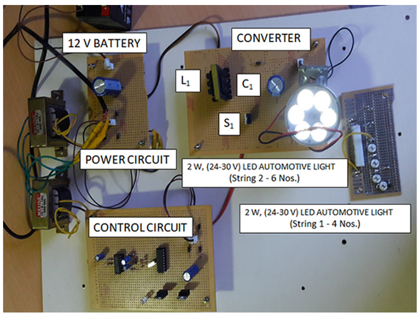

Fig. 11. Experimental setup.

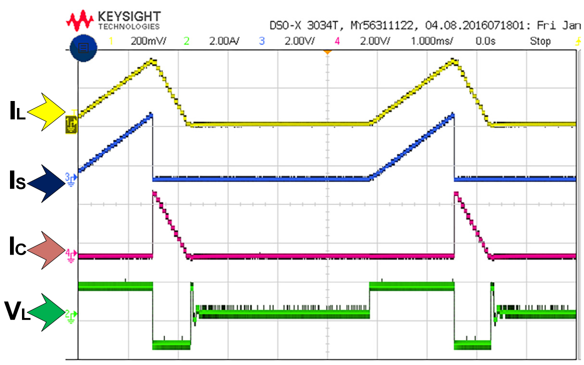

Fig. 10. Experimental waveforms for voltage mode integrated droop driver: Currents through capacitor (IC), inductor (IL), switch (IS) and voltage across inductor (VL).

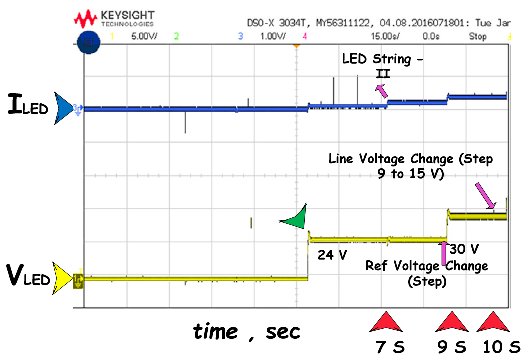

Fig. 12. Experimental waveforms for voltage mode integrated droop driver: Voltages and currents under line and load transients.

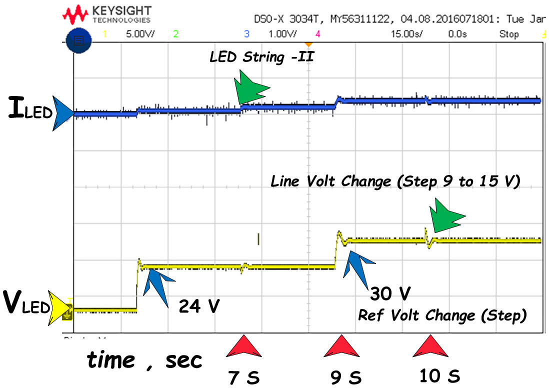

Fig. 13. Experimental waveforms for current mode integrated droop driver: Voltages and currents under line and load transients.

4. CONCLUSION

This article aims to present and prove the several reasons why the boost converter is the most popular choice for LED drivers. CDPI and CPI controllers were applied to the transformer-less types of fundamental DC converters connected to an LED load. All the converters were run in boost mode for the same simulation set up of 15/48 V and 200 mA with the controller parameter settings kept unchanged. With its large ripple content, the zeta converter is eliminated from the choice of being the LED driver. The boost converter is found to be the best in its performance under all modes of operation-current and voltage modes with CDPI. A conventional PI controller exhibits poor dynamism. The multiple perturbation analysis with step variation in the input side voltage proved that the CPI boost based LED circuit fails to recover stable conditions, unlike CDPI. The quicker settling time and rise time, the minimal overshoot, fast recovery to stable steady-state, and load transient response time, ripple-free currents and constant voltage make CDPI-V mode, the better option for an LED driver. Experimental analysis with OPAL RTDS HIL simulator validates the simulation results.

REFERENCES

Alonso, J.M.A., Perdig, M.S., Costa, M.A.D., Martinez, G., & Osorio, R. (2017). Analysis and Experiments on a Single Inductor Half Bridge LED Driver with Magnetic Control. *IEEE Transactions on Power Electronics*, volume (32), 9179-9190.

Basso, C.P. (2003). Switched Mode Power Supplies. McGraw Hill, USA.

Braitor, A.C., Konstantopoulos, C., & Kadirkamanathan, V. (2021). Current Limiting Droop Control Design annd Stability Analysis for Paralleled Boost Converters in DC Micro grids. *IEEE Transactions on Control Systems Technology*, volume (29), 100-110

Chen, W.L., Yang, C.H., Lin, C.T., Xui, M.S., & Chen, K.F. (2020). Voltage Modulation and Current Control of Boost Inverters for Stand-alone or Grid Tied Operation. *IEEE Transactions on Power Electronics*, volume (35), 8726-8736.

Czarkowsk, D. (2011). P*ower Electronics Handbook-Circuits and Applications*. Butterworth-Heinmann Publications, Elsevier,USA.

El Aroudi, A., Al Numay, M.,Haroun, R., & Zhang, G. (2021). Analytical Determination of Fast-Scale Instability Boundaries for Current Mode Controlled DC-DC Converters with CPL and Closed Voltage Loop. *IEEE Journal on Emerging and Selected Topics in Circuits and Systems*, Early Access.

Erickson, R., and Maksimovic, D. (2001). Fundamentals of Power Electronics Circuits. Kluwer Academic, USA.

Ghanbari, N., & Bhattacharya, S. (2020). Adaptive Droop Control Method for Suppressing Circulating Currents in DC Micro grid. *IEEE Open Access Journal of Power and Energy*, volume (7), 100-110

Kannan, S.S., Vijayakumar, K., and Ramanujam, R. (2016). Power Electronic Interface (PEI) Based Power Flow Control for Micro-Grid Environment -A Review. *Proceedings of the International Conference on Computation of Power, Energy, Information and Communication*, 376-380.

Lamar, D.G., Arias, M., Rodriguez, A.,Fernandez, A., Hernando, M.M., and Sebastian, J., (2013). Design Oriented Analysis and Performance Evaluation of a Low Cost High Brightness LED Driver Based on Fly-Back Power Factor Corrector. *IEEE Transactions on Industrial Electronics*, volume (60), 2614-2626.

Lamar, D.G., Zuriga, J.S., Alonso, A.R., Gonzalez, M.R., & Rezg, N. (2009). A Very Simple Control Strategy for Power Factor Correctors Driving High Brightness LEDs. *IEEE Transactions on Power Electronics*, volume (24), 2032-2042.

Li, Y., Vannorsdel, K.R., Zirger, A.J., Norris, M., and Maksimovic, D. (2012). Current Mode Control for Boost Converters with Constant Power Loads. *IEEE Transactions on Power Electronics*, volume (59), 198-206.

Mammano, R. (1999). Switching Power Supply Topology: Voltage Mode vs. Current Mode. *Application Notes of Texas Instruments*, 1-7.

Mohan, N., Undeland, T.M., and Robbins, W.P. (2010). Power Electronics: Converters, Applications and Design. Wiley Sons.

Moon, S.C., Koo, G.B.K., & Moon, G.W., (2013). A New Control Method of Interleaved Single-Stage Fly-Back AC-DC Converter for Outdoor LED Lighting Systems. *IEEE Transactions on Power Electronics*, volume (28), 4051-4062.

Mujjalinvimut, E., Ayudhya, P.N.N., & Sangswang, A. (2016). An Improved Asymmetrical Half-Bridge Converter with Self-Driven Synchronous Rectifier for Dimmable LED Lighting. *IEEE Transactions on Industrial Electronics*, volume (63), 913-925.

Peyghami, S., Pooya Davari, Mokthari, N., Loh, P.C., and Blaabjerg, F. (2017). Synchronverter Enabled DC Power Sharing Approach for LVDC Microgrids. *IEEE Transactions on Power Electronics*, volume (32), 8089-8099.

Rashid, M.H. (2003). Power Electronics Circuits Devices and Applications. Pearson Prentice Hall,USA.

Subha Sharmini K. (2019). A Simplified Pulse Generation Control Algorithm Based Upon the Concept of Synchronverter. *Part of the Advances in Intelligent Systems and Computing Book Series*, 978-981.

Wang, Q., Li, T., & Hua, Q. (2014). Dimmable and Cost-Effective DC Driving Technique for Flicker Mitigation in LED Lighting. *Journal of Display Technology*, volume (10), 766-774.

Winder, S. (2008). *Power Supplies for LED Driving*. Newnes,USA

White, B., Wang, H.L., Liu, Y.F., & Liu, X. (2015). An Average Current Modulation Method for Single-Stage LED Drivers with High Power Factor and Zero Low-Frequency Current Ripple. *IEEE Journal of Emerging and Selected Topics in Power Electronics*, volume (3), 714-731.

Wu, H., Wong, S.C., Tse, C.K., Hui, S.Y.R., & Chen, Q. (2018). Single Phase LED Drivers with Minimal Power Processing, Constant Output Current, Input Power Factor Correction, and Without Electrolytic Capacitor. *IEEE Transactions on Power Electronics*, volume (33), 6159-6170.

Zhang, Y., Qu, X., Tang, M.,Yao, R., & Chen, W. (2021). Design of Nonlinear Droop Control in DC Micro grid for Desired Voltage Regulation and Current Sharing Accuracy. *IEEE Journal on Emerging and Selected Topics in Circuits and Systems*, Early Access.

Zhong, Q.C., and Hornik, T. (2013). *Control of Power Inverters in Renewable Energy and Smart Grid*. IEEE Press, USA.